Journal of Visualized Experiments

Microfluidic model to mimic initial event of neovascularization

--Manuscript Draft--

Article Type:	Invited Methods Collection - Author Produced Video
Manuscript Number:	JoVE62003R2
Full Title:	Microfluidic model to mimic initial event of neovascularization
Corresponding Author:	Xiao Liu, Ph.D. BeiHang University School of Biological Science and Medical Engineering beijing, beijing CHINA
Corresponding Author's Institution:	BeiHang University School of Biological Science and Medical Engineering
Corresponding Author E-Mail:	liuxiao_33101128@163.com
Order of Authors:	Ping Zhao
	Xiao Liu, Ph.D.
	Xing Zhang
	Li Wang
	Haoran Su
	Liyi Wang
	Dongrui Zhang
	Xiaoyan Deng
	Yubo Fan
Additional Information:	
Question	**Response**
Please indicate whether this article will be Standard Access or Open Access.	Standard Access (US$1200)
Please specify the section of the submitted manuscript.	Bioengineering
Please confirm that you have read and agree to the terms and conditions of the author license agreement that applies below:	I agree to the Author License Agreement
Please provide any comments to the journal here.	
Please indicate whether this article will be Standard Access or Open Access.	Standard Access ($1400)

TITLE:

Microfluidic Model to Mimic Initial Event of Neovascularization

AUTHORS AND AFFILIATIONS:

Ping Zhao[1], Xing Zhang[1], Xiao Liu[1], Li Wang[4], Haoran Su[1], Liyi Wang[1], Dongrui Zhang[1], Xiaoyan Deng[3], Yubo Fan[1,2]

[1]Beijing Advanced Innovation Centre for Biomedical Engineering, Key Laboratory for Biomechanics and Mechanobiology of Chinese Education Ministry, School of Biological Science and Medical Engineering, Beihang University, Beijing, China
[2]School of Engineering Medicine, Beihang University, Beijing, China
[3]Artificial Intelligence Key Laboratory of Sichuan Province, School of Automation and Information Engineering, Sichuan University of Science and Engineering，Zigong, Sichuan, China
[4]Beijing Research Center of Urban System Engineering, Beijing, China

Email Addresses of co-authors:

Ping Zhao	(pingzhao1007@163.com)
Xing Zhang	(zhangxing9519@163.com)
Li Wang	(wangli@xtgc.org.cn)
Haoran Su	(13261677588@163.com)
Liyi Wang	(iswangly@buaa.edu.cn)
Dongrui Zhang	(zhangdr0306@126.com)
Xiao Liu	(liuxiao@buaa.edu.cn)
Xiaoyan Deng	(dengxy1953@buaa.edu.cn)
Yubo Fan	(yubofan@buaa.edu.cn)

Correspondence to:

Xiao Liu	(liuxiao@buaa.edu.cn)
Xiaoyan Deng	(dengxy1953@buaa.edu.cn)
Yubo Fan	(yubofan@buaa.edu.cn)

KEYWORDS:

neovascularization, microfluidics, shear stress, microenvironment, transendothelial flow, 3D culture

SUMMARY:

Here, we provide a microfluidic chip and an automatically controlled, highly efficient circulation microfluidic system that recapitulates the initial microenvironment of neovascularization, allowing endothelial cells (ECs) to be stimulated by high luminal shear stress, physiological level of transendothelial flow, and various vascular endothelial growth factor (VEGF) distribution simultaneously.

ABSTRACT:

Neovascularization is usually initialized from an existing normal vasculature and the

biomechanical microenvironment of endothelial cells (ECs) in the initial stage varies dramatically from the following process of neovascularization. Although there are plenty of models to simulate different stages of neovascularization, an *in vitro* 3D model that capitulates the initial process of neovascularization under the corresponding stimulations of normal vasculature microenvironments is still lacking. Here, we reconstructed an *in vitro* 3D model that mimics the initial event of neovascularization (MIEN). The MIEN model contains a microfluidic sprouting chip and an automatic control, highly efficient circulation system. A functional, perfusable microchannel coated with endothelium was formed and the process of sprouting was simulated in the microfluidic sprouting chip. The initially physiological microenvironment of neovascularization was recapitulated with the microfluidic control system, by which ECs would expose to high luminal shear stress, physiological transendothelial flow, and various vascular endothelial growth factor (VEGF) distributions simultaneously. The MIEN model can be readily applied to the study of neovascularization mechanism and holds a potential promise as a low-cost platform for drug screening and toxicology applications.

INTRODUCTION:

Neovascularization happens in many normal and pathological processes[1–4], which include two major processes in adults, angiogenesis and arteriogenesis[5]. Besides the best-known growth factors, such as vascular endothelial growth factor (VEGF)[6], mechanical stimulations, in particular the blood flow induced shear stress is important in the regulation of neovascularization[7]. As we know, the magnitude and forms of shear stress vary dramatically and dynamically in different parts of the vasculature, resulting in important effects on vascular cells[8–12]. Previous studies have shown that shear stress may affect various aspects of ECs, including cell phenotypic changes, signal transduction, gene expression, and the communication with mural cells[13–20]; hence, regulate neovascularization[21–24].

Therefore, to better understand neovascularization, it is important to reconstruct the process in natural cellular microenvironment *in vitro*. Recently, many models have been established to create micro-vessels and provide precise control of microenvironment[25–27], taking advantage of advances in microfabrication and microfluidic technology. In these models, micro-vessels can be generated by hydrogel[28,29], polydimethylsiloxane (PDMS) microfluidic chips[30–32] or 3D bioprinting[33,34]. Some aspects of the microenvironment, such as luminal shear stress[22,23,35,36], transendothelial flow[37–40], biochemical gradient of angiogenic factors[41,42], strain/stretch[43–45], and co-cultured with other types of cells[32,46] have been mimicked and controlled. Usually, a large reservoir or syringe pump was used to provide perfused medium. Transendothelial flow in these models was created by pressure drop between the reservoir and micro-tube[22,23,38,40]. However, the mechanical microenvironment is hard to maintain constantly in this way. Transendothelial flow would increase and then exceed the physiological level if a high flow rate with high shear stress was used for perfusion. Previous study showed that at the initial period of neovascularization, the velocity of transendothelial flow is very low due to the intact ECs and basement membrane, usually under 0.05 μm/s[8]. Meanwhile, though luminal shear stress in vascular system varies greatly, it is relatively high with mean values of 5–20 dyn/cm^2[–11,47]. For now, the velocity of transendothelial flow in previous works have been generally kept between 0.5–15 μm/s[22,38-40], and the luminal shear stress was usually under 10 dyn/cm^2 [23]. It remains a

difficult subject to constantly expose ECs to high luminal shear stress and physiological level of transendothelial flow simultaneously.

In the present study, we describe an *in vitro* 3D model to mimic the initial event of neovascularization (MIEN). We developed a microfluidic chip and an automatic control, highly efficient circulation system to form perfusion micro-tubes and simulate the process of sprouting[48]. With the MIEN model, the microenvironment of ECs stimulated at the initial period of neovascularization are firstly recapitulated. ECs can be stimulated by high luminal shear stress, physiological level of transendothelial flow and various VEGF distribution simultaneously. We describe the steps of establishing the MIEN model in detail and the key points to be paid attention to, hoping to provide a reference for other researchers.

PROTOCOL:

1. Wafer preparation

NOTE: This protocol is specific for the SU-8 2075 negative photoresist used during this research.

1.1. Clean the silicon wafer 3 to 5 times with methanol and isopropanol on a spin coater as follows: first spin for 15 s at 500 rpm, then spin for 60 s at 3,000 rpm.

1.2. Transfer the silicon wafer to a hotplate, which preheated to 180 °C and bake the wafer for 10 min.

1.3. Remove the silicon wafer from the hotplate and cool it to room temperature. Clean the wafer again with compressed air before proceeding with the spin coating. Apply 4 mL of the SU-8 2075 photoresist to the center of the wafer.

1.4. Obtain a feature height of 70 µm on the spin coater as follows: first spin for 12 s at 500 rpm, then spin for 50 s at 2,100 rpm.

1.5. Soft bake the wafer on a hotplate as follows: first bake for 8 min at 65 °C, then bake for 20 min at 95 °C. Next, remove the silicon wafer from the hotplate and cool it to room temperature before lithography.

1.6. Place a photomask onto the photoresist film. Expose the wafer with a lithography equipment to achieve a total exposure of 200 mJ/cm^2.

NOTE: The photomask contains nine sets of patterns of the chip, so it can fabricate nine microfluidic sprouting chips each time.

1.7. Post exposure the wafer on a hotplate as follows: first bake for 5 min at 65 °C, then bake for 20 min at 95 °C. Next, remove the silicon wafer from the hotplate and cool it to room temperature before developing.

1.8. Transfer the wafer to a glass Petri dish filled with SU-8 developer (PGMEA) to start developing.

CAUTION: The developer is irritating to the eyes and respiratory tract. Perform developing in a fume hood. Wear splash goggles, nitrile gloves, and airline mask during the operation.

1.9. Shake the dish gently along the direction of the flow channel and change the developer after 10 min.

1.10. Repeat step 1.9 for 3–5 times until the patterns can be clearly observed.

NOTE: Make sure there is no photoresist residue left on the wafer, otherwise rinse the wafer in the developer again.

1.11. Transfer the wafer to a preheated hotplate set to 120 °C and bake it for 30 min.

1.12. Pipet 35 µL of silane onto a coverslip, then put the coverslip along with the wafer into a desiccator and pull vacuum. Seal the desiccator and leave the wafer under vacuum for 4 h to silanize the wafer to prevent the adhesion of PDMS during the soft-lithography processes.

CAUTION: The silane is toxic. To prevent poisoning, perform silanization in the fume hood and wear nitrile gloves while handling.

1.13. Release the vacuum from the desiccator. Remove the silanized wafer onto a preheated hotplate and bake it at 65 °C for 2 h.

1.14. Store the wafer in a clean Petri dish until required.

2. Microfluidic sprouting chip fabrication

2.1. Combine 20 g of base agent and 2 g of curing agent (10:1 ratio) in a plastic beaker and mix them thoroughly with a mixing rod.

2.2. Place the beaker into a desiccator and pull vacuum for 1 h to remove air bubbles in the PDMS mixture.

2.3. Pour the PDMS mixture onto the wafer in the Petri dish and place the Petri dish back into the desiccator, degassing for another 30 min.

NOTE: It is helpful to use double-sided adhesive tape to glue the wafer onto the bottom of the Petri dish to ensure the wafer is kept horizontal during degassing and curing.

2.4. Remove the Petri dish from the desiccator and place it into an 80 °C dry oven for 3 h to

cure.

2.5. Carefully separate the PDMS layer from the wafer and cut the layer to nine chips with a scalpel according to the pattern.

NOTE: Keep the feature side up after separation.

2.6. Punch two hydrogel injection ports and four media injection ports out of each chip using a 1 mm and a 3.5 mm biopsy punch, respectively.

2.7. Clean the punched chips with residue-free tape to remove PDMS residue. Place the chips and nine glass coverslips into a plasma cleaner and treat them with oxygen plasma for 30 s to form covalent bonding on the surface.

2.8. Take out the chips and coverslips. Attach the feature side of the chips onto the coverslips.

2.9. Place the attached chips into an 80 °C dry oven for 1 h to intensify the bonding.

2.10. Autoclave the chips before use and keep them sterile for the rest of the procedure.

3. Surface modification and hydrogel injection

3.1. For each chip, pipet 40 µL of 1 mg/mL poly-D-lysine (PDL) and inject it into channels in the chip from hydrogel injection port.

NOTE: Make sure the PDL fills channels, especially in narrow channels near the ports.

3.2. Incubate the chips at 37 °C for 4 h to modify the surface of the PDMS .

3.3. Pipet 200 µL of sterile water and inject it into channels in the chip from hydrogel injection port to wash out PDL.

3.4. Remove the chips into a 120 °C dry oven for 3 h to restore hydrophobicity.

3.5. Place on ice a sterile tube and calculate the volume of Type I collagen to be used as the following equation.

Final volume (50 µL) x Final collagen concentration (3 mg/mL in this research) /
Concentration in bottle = volume collagen to be added

3.6. Calculate the volume of NaOH to be used as the following equation.

(volume collagen to be added) x 0.023 = volume 1 N NaOH

3.7. Prepare 50 µL of hydrogel in the tube as the following protocol: add 5 µL of 10x PBS, 0.5 µL of phenol red, calculated volume of 1 N NaOH, 4 µL of 1 mg/mL Fibronectin, calculated volume

of Type I collagen in turn. Add proper amount of dH_2O so that the total volume reaches 50 µL. Mix all the contents in the tube thoroughly.

NOTE: Perform all the operations on ice. Use phenol red as an acid-based indicator to assist in visual determination of the pH of the hydrogel. The final hydrogel ends up orange when the pH is about 7.4 and the stiffness is about 15 kPa[49].

3.8. Pipet 2–3 µL of hydrogel for each chip and slowly inject it into the central hydrogel channel from hydrogel injection port.

3.9. Incubate the chips at 37 °C for 30 min to allow gelation.

NOTE: Seal the chips into a sealed box with 1 mL of sterile water if they are not used immediately. Sealed chips can be stored at 37 °C for at most 24 h.

4. Cell seeding

4.1. Pipet 20 µL of 125 µg/mL Fibronectin into one media injection port of the cell culture channel.

4.2. Cut a pipette tip to fit the port of the cell culture channel with scissors.

4.3. Insert the pipette tip into the other media injection port of the cell culture channel. Then, pipet out air from the cell culture channel to fill it with Fibronectin.

4.4. Incubate the chips at 37 °C for 1 h.

4.5. Before cell seeding, pipet 20 µL of ECM media into each media injection port and incubate the chips at 37 °C for 30 min.

4.6. Then, pipet out all the media in all media injection ports.

4.7. Next, pipet 5 µL of cell suspension into one media injection port of cell culture channel. Then, endothelial cells quickly spread over the entire channel under differential hydrostatic pressure.

NOTE: Prepare the cell suspension by trypsinizing human umbilical vein endothelial cells (HUVECs) from the culture flask and centrifuging them at 400 x *g*. Then, resuspend the cells to 10^7 cells/mL in a tube.

4.8. Add about 4–6 µL of ECM media to the other port to adjust the hydrostatic pressure and stop cell moving.

4.9. Remove the chips to the cell incubator. Then, turn over the chips every 30 min until

endothelial cells coat around the internal surface of the cell culture channel 2 h later (**Figure 1**).

NOTE: To make the chip upside down, pipet a little water on the back of the coverslip then the chip can attach to the cover of the Petri dish.

4.10. Use the pipette tip to remove the attached cells in the injection ports very carefully.

4.11. Then, insert four barbed female Luer adaptors into the media injection ports and fill with ECM media.

NOTE: The adaptors can function as fluid reservoirs to provide nutrients for the cells in the channel.

4.12. Remove the chips to cell incubator. Change ECM media in Luer adaptors every 12 h.

5. Measurement of FITC-dextran diffusional permeability

NOTE: To assess barrier function of the micro-vessel, diffusional permeability of the EC culture channel with or without cell lining is assessed.

5.1. Take out a microfluidic sprouting chip with hydrogel injected.

5.2. Repeat steps 4.1–4.6.

5.3. Remove all the Luer adaptors and pipet out all the media in four media injection ports.

5.4. Place the chip onto the confocal laser scanning microscope.

5.5. Pipet 5 µL of culture media containing 500 µg/mL 40 kDa FITC-dextran to one port of cell culture channel.

NOTE: 40 kDa FITC-dextran has similar molecular size to VEGF-165 (39–45 kDa).

5.6. Capture images every 3 s for 30 s. Thus, the diffusional permeability without cell lining is measured.

5.7. Take out microfluidic sprouting chip after HUVECs are confluent in the cell culture channel.

5.8. Repeat steps 5.3–5.5.

5.9. Capture images every 3 s for 30 s. Thus, the diffusional permeability with cell lining is measured.

5.10. Calculate the diffusional permeability by quantifying changes of fluorescent intensity over time using the following modified equation[50].

$$P_d = (I_2 - I_1) / ((I_1 - I_b)\cdot\triangle t) \cdot S/d$$

where, P_d is diffusional permeability coefficient, I_1 is average intensity at an initial time point, I_2 is average intensity after delta time ($\triangle t$), I_b is background intensity, S is the area of the channel in fluorescence images, and d is the total interval of micro-posts in fluorescence images. In the present work, $\triangle t$ is set as 9 s.

NOTE: The present equation is slightly different from the original[50], due to the diffusion direction of the fluorescence in the chip is only from the EC channel to hydrogel channel, which is not like the circular tube diffusing in all the radial direction.

6. Microfluidic control system setup

NOTE: The microfluidic control system in the present study is consisted of a micro-syringe pump, an electromagnetic pinch valve, a bubble trap chip, a microfluidic chip, a micro-peristaltic pump, and a reservoir. Each part of the system can be replaced by alternatives able to perform the same function.

6.1. Bubble trap chip fabrication

NOTE: The bubble trap chip is used to remove air bubbles in circulation. The chip consists of three PDMS layers. The top layer is constructed using soft lithography to form grid structure as the liquid chamber. Each channel of the grid structure is 100 µm wide. The bottom layer is a PDMS chunk with a hole. Between the two layers, a 100 µm thin PDMS film is laid.

6.1.1. Repeat step 1 to prepare the wafer for bubble trap chip.

6.1.2. Repeat steps 2.1–2.5 to fabricate the top layer and bottom layer of the bubble trap chip.

NOTE: The photomask of the top layer contains three sets of patterns, so cut the PDMS layer to three chips according to the pattern.

6.1.3. Punch six holes on the end of inlet and outlet channels of the top layer using a 3.5 mm biopsy punch.

6.1.4. Punch two holes on the corresponding position of bottom layer using a 6 mm biopsy punch according to the pattern on the top layer.

6.1.5. Repeat steps 2.1–2.2 to prepare 10 g of PDMS mixture and pour it on the center of a cleaned silicon wafer.

6.1.6. Fabricate a 100 µm PDMS film by applying the following spin protocol: spin for 15 s at 500 rpm, increase the spin speed to 1,300 rpm and hold here for 45 s.

6.1.7. Transfer the wafer to a preheated hotplate set to 180 °C and bake it for 30 min.

6.1.8. Clean the punched layers with residue-free tape to remove PDMS residue. Place the top layers and wafer into a plasma cleaner and treat them with oxygen plasma for 30 s to form covalent bonding on the surface.

6.1.9. Take out top layers and wafer. Attach the feature side of top layers onto the PDMS film.

6.1.10. Cut the film carefully along the edge of the top layers with a needle.

6.1.11. Slowly separate the film from the wafer and turn over the chips to make the film side up after separation.

6.1.12. Place the bottom layers and attached chips into a plasma cleaner and treat them with oxygen plasma for 30 s again.

6.1.13. Take out bottom layers and attached chips. Attach the bottom layers onto the PDMS film and the bubble trap chips are done.

NOTE: Align the holes on the bottom layer with the patterns on the top layer when attaching.

6.1.14. Place the chips into an 80 °C dry oven for 1 h to intensify the bonding.

6.2. Assemble the microfluidic control system

NOTE: All the parts of the system, such as bubble trap chip, reservoir, tubes, and connectors are used after autoclave sterilization, except electronic equipment. Assemble the microfluidic control system on a clean bench.

6.2.1. To assemble the microfluidic control system, prepare two polytetrafluoroethylene tubes, two short silicone tubes, three long silicone tubes, one barbed female Luer adaptor, one Y type connector, and three L type connectors.

NOTE: The advantage of polytetrafluoroethylene tube is low elasticity, therefore, less media is needed in pipeline. Silicone tube, in contrast, has high elasticity, therefore, it is suitable for the pinch valve and peristaltic pump.

6.2.2. Fill the syringe with 10 mL of preheated (37 °C) ECM medium.

NOTE: Preheating helps the medium release dissolved gas.

6.2.3. Connect a polytetrafluoroethylene tube to the syringe by a barbed female Luer adaptor. Then, connect the other end of polytetrafluoroethylene tube to a Y type connector.

6.2.4. Next, connect two long silicone tubes to the other two ends of Y type connector with one tube connecting to the reservoir and the other tube connecting to the bubble trap chip.

6.2.5. Connect another long silicone tube to the reservoir.

6.2.6. Next, use two short silicone tubes to connect all inlet and outlet holes on the top layer of the bubble trap chip. Connect a polytetrafluoroethylene tube to the backend of the chip.

6.2.7. Next, fix the syringe onto the micro-syringe pump.

6.2.8. Clip two long silicone tubes into the electromagnetic pinch valve.

6.2.9. Next, switch the electromagnetic pinch valve to open the pipeline between the syringe and the reservoir. Inject the media to the reservoir using a micro-syringe pump to exhaust air in the tube.

6.2.10. Then, switch the valve again to open the pipeline between the syringe and the bubble trap chip. Inject the media to fill the liquid chamber and the backend tube of the bubble trap chip.

7. Endothelial sprouting assay

NOTE: A stage top incubator assembled with phase contrast microscope is used in the present study to observe the process of sprouting in real time. The stage top incubator can maintain the temperature, humidity, and CO_2 control on microscope stages, being good for live cell imaging. But the equipment is not necessary for the assay. The protocols provided here can also be worked in a basic cell incubator.

7.1. Take out endothelial sprouting chips from the cell incubator.

7.2. Then, remove Luer adaptors on the cell culture side. Insert two pipe plugs into the hydrogel injection ports of the microfluidic sprouting chip.

NOTE: The plugs can transform from needles and their main function is to prevent media from spilling.

7.3. Connect the backend tube of bubble trap chip to one port of cell culture channel.

NOTE: Make sure there are no bubbles in the tube before connection.

7.4. Insert a T type connector to the other port and connect it to long silicone tube connected with the reservoir.

7.5. Clip the long silicone tube into the micro-peristaltic pump.

7.6. Then, insert an air filter to the reservoir.

7.7. Next, assemble the microfluidic sprouting chip to the stage top incubator.

7.8. Next, connect the vacuum pump to the holes in the bottom layer of bubble trap chip by a TPU tube.

7.9. Set up the circulation volume and flow rate in the custom program which controls the micro-syringe pump and electromagnetic pinch valve simultaneously (**Figure 2**).

NOTE: The flow rate across the endothelial cell culture channel is calculated according to the classic equation.

$$\tau = 6\mu Q / Wh^2$$

where, τ is shear stress (dyn/cm^2), μ is viscosity of the medium (8.8 x 10^{-4} Pa · s), Q is the flow rate across the endothelial cell culture channel (ml/s), *h* is channel height (70 μm), and W is channel width (1,000 μm). The viscosity of the medium is measured using a coaxial cylinder type rotational viscometer. The height and width of the channel are predetermined and manually confirm using a phase contrast microscope at 4x magnification. The circulation volume is 5 mL and flow rate is 85 μL/min (average 0.2 m/s in cell culture channel) for 15 dyn/cm^2 shear stress according to calculation.

7.10. Next, set up the flow rate of micro-peristaltic pump.

NOTE: The flow rate of micro-peristaltic pump is slightly higher than micro-syringe pump, in order to prevent the media from spilling.

7.11. Turn on the micro-syringe pump. Then, the circulation control system is established.

8. Data analysis

NOTE: To quantify the sprouts, the normalized area of sprouting, average sprout length, and longest sprout length were calculated. Results represent mean ± SEM obtained from three independent studies. Statistical significance ($P < 0.05$) is assessed by Student's *t*-test.

8.1. Fix cells and sprouts in the microfluidic sprouting chip after experiments with 4% paraformaldehyde in PBS for 15 min. Stain nuclei with 4',6-diamidino-2-phenylindole dihydrochloride (DAPI; 1: 1000; Sigma-Aldrich) for 10 min and then stain cytoskeleton with TRITC phalloidin (P5285, 1: 100; Sigma-Aldrich) for 1 h. Wash cells with PBS three times at 5 min intervals between each step.

8.2. Take confocal images of the chips in a tiling mode and stitch them using image editing software.

8.3. Count the number of fluorescent pixels of Z-projection images using a custom code in programming software to quantify normalized area of sprouting (See **Supplemental File**).

8.4. Manually identify and label each tip of sprouts in Z-projection images and calculate distances between sprouts tips to ECs basement membrane using another custom code to quantify average sprout length and longest sprout length (See **Supplemental File**).

REPRESENTATIVE RESULTS:

The *in vitro* 3D model to mimic the initial event of neovascularization (MIEN) presented here consisted of a microfluidic sprouting chip and a microfluidic control system. The microfluidic sprouting chip was optimized from previous publications[22,23,37,40,51–53]. Briefly, it contained three channels and six ports: an endothelial cell culture channel and a liquid channel with four media injection ports, and a central hydrogel channel with two hydrogel injection ports (**Figure 3**). The microfluidic control system consisted of a micro-syringe pump, an electromagnetic pinch valve, a bubble trap chip, a micro-peristaltic pump, and a culture medium reservoir (**Figure 4**). A custom program was used to control the micro-syringe pump and electromagnetic pinch valve simultaneously, with which the flow rate and circulation volume can be set up. A compensation volume was introduced to correct the slight change of volume after multiple cycles due to systemic error. To minimize the medium used for perfusion, an electromagnetic pinch valve was introduced for medium recycle. The electromagnetic pinch valve could switch between two states to make the microfluidic system in two phases in a cycle. In the injection phase, culture medium was slowly injected from the micro-syringe pump to the microfluidic sprouting chip. While in the recycle phase, culture medium was very rapidly extracted from the reservoir back to the micro-syringe pump.

The barrier function of the micro-vessel in our MIEN model was assessed by measuring the diffusional permeability coefficient (P_d) of 40 kDa FITC-dextran. As it is shown in **Figure 5**, the P_d of static cultured chip with cell lining is 0.1 ± 0.3 µm/s, and the P_d of empty channel without cell lining is 5.4 ± 0.7 µm/s. Then, endothelial sprouting assay under static and perfusion was performed in the MIEN model. In static conditions, endothelial sprouting occurred about 4 h after seeding and the sprouts would migrate across the central hydrogel channel to the other side in about 48 h. The sprouts degraded gradually after 48 h. While after 24 h of exposure to 5 or 15 dyn/cm^2 shear stress (average 0.07 or 0.2 m/s in cell culture channel), ECs aligned in the flow direction changing from polygonal, cobblestone shape into fusiform, and the degree of sprouting decreased with the increase of shear stress (**Figure 6**). However, the sprouts under shear conditions were more stable than under static culture conditions. They could maintain over 48 h under perfusion. Quantitative statistics showed that endothelial sprouting decreased significantly in terms of area of sprouting, average sprout length, and longest sprout length (**Figure 7**).

FIGURE AND TABLE LEGENDS:

Figure 1: Endothelial cells coat around the internal surface of the cell culture channel. HUVECs

are evenly dispersed in the cell culture channel 2 h after cell seeding.

Figure 2: The custom program used to control the micro-syringe pump and electromagnetic pinch valve simultaneously. Main page (up) and subpage (down) of the custom program with which the flow rate and circulation volume can be set up. A compensation volume was introduced to correct the slight change of volume after multiple cycles due to systemic error.

Figure 3: The schematic of the microfluidic sprouting chip. The chip contains three channels and six ports: an endothelial cell culture channel and a liquid channel with four media injection ports, and a central hydrogel channel with two hydrogel injection ports.

Figure 4: The schematic of the microfluidic control system. The microfluidic control system consists of a micro-syringe pump, an electromagnetic pinch valve, a bubble trap chip, a micro-peristaltic pump, and a culture medium reservoir.

Figure 5: Diffusional permeability (P_d) of 40 kDa FITC-dextran. The P_d of static cultured chip with cell lining is 0.1 ± 0.3 μm/s, and the P_d of empty channel without cell lining is 5.4 ± 0.7 μm/s. **, $p < 0.01$.

Figure 6: Representative images of endothelial sprouting under different shear conditions. After 24 h of static culturing, HUVECs invade from the cell culture channel into the adjacent hydrogel channel through micro-posts and a large number of sprouts in the hydrogel. While after 24 h of exposure to 5 or 15 dyn/cm^2 shear stress, the degree of sprouting decrease obviously.

Figure 7: Quantified area of sprouting, average sprout length, and longest sprout length. After 24 h of static culture (S0) or exposure to 5 (S5) or 15 (S15) dyn/cm^2 shear stress, the degree of sprouting decrease with the increase of shear stress. *, $p < 0.05$; **, $p < 0.01$.

DISCUSSION:

For a long time, real-time observation of neovascularization has been a problem. Several approaches have been developed recently to create perfused vessels lining with ECs and adjacent to extracellular matrix for sprouting[22,32,40,46,54], but the mechanical microenvironment is still hard to maintain constantly. It remains a difficult subject to mimic the initial biomechanical microenvironment of ECs, which are subjected to high luminal shear stress and low velocity of transendothelial flow. Here, we presented a MIEN model that firstly simulates the initial event of neovascularization in mimic physiological microenvironment. With the MIEN model, automatic, efficient and bubble-free long-term perfusion is achieved. Luminal shear stress on ECs could be optionally changed at any time during experiments with transendothelial flow staying at physiological level.

The key of the MIEN model is decoupling the effect of luminal flow on ECs from transendothelial flow. To this end, a T-type connector is creatively inserted to the outlet port of the EC culture channel. One end of the connector is connected to the reservoir through the micro-peristaltic pump. The other end of the connector is exposed to the air of the incubator. It keeps pressure

inside the endothelial cell culture channel the same as the atmospheric pressure, since there is neither surplus media gathering to increase pressure nor excess media being drawn away to form negative pressure in the channel. In this way, the flow resistance after microfluidic sprouting chip is very small so that the transendothelial flow can be maintained at physiological range even under high luminal shear stress.

One critical step within the protocol is the successful injection of hydrogel in central hydrogel channel. Huang et al. proposed that successful filling of the gels depends on balancing the capillary forces and surface tension within the microfluidic gel channel[55]. They found three different variables to control the balance: the spacing between micro-posts, the surface properties of the device, and the viscosity of the hydrogel precursor solutions. In the present model, the design of the microfluidic sprouting chip is optimized from previous works[22,23,37,40,51–53]. The geometry and spacing of micro-posts to separate three channels are determined based on previous calculations and numerous experiments. Further, PDL coating and high temperature baking are performed to modify the PDMS surface; hence, adjust the balance between hydrophilicity and hydrophobicity before hydrogel injection.

The other critical step of the protocol is the removal of bubbles. A large amount of air will dissolve into circulation medium during the experiment due to the T-type connector and micro-peristaltic pump, resulting in bubbles in circulation and greatly affecting the function of endothelial cells. To remove bubbles, a bubble trap chip is introduced before microfluidic sprouting chip. It works based on the high gas permeability of the PDMS membrane. When bubbles get into the trap, they are dispersed by the small and dense grid structure and trapped due to the negative pressure generated by the vacuum pump so that they fail to move forward into the microfluidic sprouting chip. Further, the bubbles transport through the PDMS membrane into the negative pressure hole connected to the vacuum pump and disappear eventually. Even so, great attention should be paid to the formation of bubbles during the experiment. As soon as bubbles are found before microfluidic sprouting chip in the pipeline, stop the micro-syringe pump immediately. Gently flinch the pipeline with the finger to let the bubbles move to bubble trap chip and be removed.

Although the initial microenvironment of neovascularization is partially recapitulated, there are some limitations to this MIEN model. The mechanical microenvironments of endothelial cells such as blood induced shear stress and extracellular matrix stiffness are changing during the neovascularization processes. Before neovascularization, the endothelial basement membrane is still intact with complete barrier function, resulting in high luminal shear stress with low velocity of transendothelial flow and interstitial flow[8,9]. At the onset of angiogenesis and arteriogenesis, a hallmark event is matrix metalloproteases (MMPs) mediation of basement degradation, which will increase ECs permeability and remodel matrix, leading to changes in mechanical microenvironments such as blood induced shear stress and extracellular matrix stiffness. In the present work, we focus on the initiation of neovascularization so the mechanical environments within the microfluidic sprouting chip are designed to keep stable to simulate the physiological conditions. However, changes of mechanical microenvironments will occur with the ECs sprouting, just like *in vivo*. Besides, similar to many previous studies[34,53,56], the present model

takes collagen hydrogel as an extracellular matrix. As we focus on the effect of flow induced shear stress, only one stiffness hydrogel is used. However, considering the important effect of matrix stiffness on cell behavior and neovascularization, different stiffnesses of collagen should be studied and can be achieved by regulating the pH of collagen since the mechanical properties of collagen is depending on its pH[49]. But it is important to note that the hydrogel needs to be thoroughly rinsed with PBS to remove residual acids or bases before cell seeding to prevent damage to the cells. Further, to mimic the complex components of ECM *in vivo*, various hydrogels such as Matrigel, hyaluronic acid (HA), and fibrinogen etc. should be used in the future to improve the present model. Blood pressure induced cyclic strain is another important hemodynamic force that modulates the morphology and functions of vascular cells[57]. Previous studies have shown that tensile strain enhanced expression of angiogenic factors in human mesenchymal stem cells[58] and induced angiogenesis via degradation of type IV collagen in the vascular endothelial basement membrane[59]. These results indicated that blood pressure induced strain may affect neovascularization too. The present model focuses on the effect of flow induced shear stress so it isn't applicable to introduce strain as the hydrogel doesn't stick tightly enough to the channel and will fall off when stretched. We will pay attention to overcome this difficulty in future works.

ACKNOWLEDGMENTS:

This work was supported by the National Natural Science Research Foundation of China Grants-in-Aid (grant nos. 11827803, 31971244, 31570947, 11772036, 61533016, U20A20390 and 32071311), National key research and development program of China (grant nos. 2016YFC1101101 and 2016YFC1102202), the 111 Project (B13003), and the Beijing Natural Science Foundation (4194079).

DISCLOSURES:

The authors have nothing to disclose.

REFERENCES:

1. Potente, M., Gerhardt, H., Carmeliet, P. Basic and therapeutic aspects of angiogenesis. *Cell*. **146** (6), 873–887 (2011).
2. Barger, A. C., Beeuwkes, R. D., Lainey, L. L., Silverman, K. J. Hypothesis: vasa vasorum and neovascularization of human coronary arteries. A possible role in the pathophysiology of atherosclerosis. *New England Journal of Medicine*. **310** (3), 175–177 (1984).
3. Homan, K. A. et al. Flow-enhanced vascularization and maturation of kidney organoids in vitro. *Nature Methods*. 16 (3), 255–262 (2019).
4. Rouwkema, J., Khademhosseini, A. Vascularization and angiogenesis in tissue engineering: beyond creating static networks. *Trends in Biotechnology*. **34** (9), 733–745 (2016).
5. Carmeliet, P. M. J. Mechanisms of angiogenesis and arteriogenesis. *Nature Medicine*. **6** (4), 389–395 (2000).
6. Yancopoulos, G. D. et al. Vascular-specific growth factors and blood vessel formation. *Nature*. **407** (6801), 242–248 (2000).
7. Heil, M., Eitenmüller, I., Schmitz‐Rixen, T., Schaper, W. Arteriogenesis versus angiogenesis: similarities and differences. *Journal of Cellular and Molecular Medicine*. **10**

(1), 45–55 (2006).
8. Tarbell, J. M., Demaio, L., Zaw, M. M. Effect of pressure on hydraulic conductivity of endothelial monolayers: role of endothelial cleft shear stress. *Journal of Applied Physiology*. **87** (1), 261 (1999).
9. Pedersen, J. A., Lichter, S., Swartz, M. A. Cells in 3D matrices under interstitial flow: Effects of extracellular matrix alignment on cell shear stress and drag forces. *Journal of Biomechanics*. **43** (5), 900–905 (2010).
10. Pries, A. R., Secomb, T. W., Gaehtgens, P. Biophysical aspects of blood flow in the microvasculature. *Cardiovascular Research*. **32** (4), 654–667 (1996).
11. Ballermann, B. J., Dardik, A., Eng, E., Liu, A. Shear stress and the endothelium. *Kidney International*. **54**, S100–S108 (1998).
12. Stone, P. H. et al. Prediction of sites of coronary atherosclerosis progression: In vivo profiling of endothelial shear stress, lumen, and outer vessel wall characteristics to predict vascular behavior. *Current Opinion in Cardiology*. **18** (6), 458–470 (2003).
13. Wragg, J. W. et al. Shear stress regulated gene expression and angiogenesis in vascular endothelium. *Microcirculation*. **21** (4), 290–300 (2014).
14. Yoshino, D., Sakamoto, N., Sato, M. Fluid shear stress combined with shear stress spatial gradients regulates vascular endothelial morphology. *Integrative Biology Quantitative Biosciences from Nano to Macro*. **9** (7), 584–594 (2017).
15. Chistiakov, D. A., Orekhov, A. N., Bobryshev, Y. V. Effects of shear stress on endothelial cells: go with the flow. *Acta Physiologica*. **219** (2), 382–408 (2016).
16. Tarbell, J. M. Shear stress and the endothelial transport barrier. *Cardiovascular Research*. **87** (2), 320–330 (2010).
17. Hergenreider, E. et al. Atheroprotective communication between endothelial cells and smooth muscle cells through miRNAs. *Nature Cell Biology*. **14** (3), 249 (2012).
18. Chien, S. Mechanotransduction and endothelial cell homeostasis: the wisdom of the cell. *American Journal of Physiology Heart & Circulatory Physiology*. **292** (3), H1209 (2007).
19. Qi, Y. X. et al. PDGF-BB and TGF-{beta}1 on cross-talk between endothelial and smooth muscle cells in vascular remodeling induced by low shear stress. *Proceedings of the National Academy of Sciences of the United States of America*. **108** (5), 1908–1913 (2011).
20. Chiu, J. J., Shu, C. Effects of disturbed flow on vascular endothelium: pathophysiological basis and clinical perspectives. *Physiological Reviews*. **91** (1), 327–387 (2011).
21. Tressel, S. L., Huang, R. P., Tomsen, N., Jo, H. Laminar shear inhibits tubule formation and migration of endothelial cells by an angiopoietin-2 dependent mechanism. *Arteriosclerosis, Thrombosis, and Vascular Biology*. **27** (10), 2150–2156 (2007).
22. Song, J. W., Munn, L. L. Fluid forces control endothelial sprouting. *Proceedings of the National Academy of Sciences of the United States of America*. **108** (37), 15342–15347 (2011).
23. Galie, P. A. et al. Fluid shear stress threshold regulates angiogenic sprouting. *Proceedings of the National Academy of Sciences of the United States of America*. **111** (22), 7968–7973 (2014).
24. Pipp, F. et al. Elevated fluid shear stress enhances postocclusive collateral artery growth and gene expression in the pig hind limb. *Arteriosclerosis, Thrombosis, and Vascular Biology*. **24** (9), 1664–1668 (2004).

25. Islam, M. M., Beverung, S., Steward, R., Jr. Bio-Inspired Microdevices that Mimic the Human Vasculature. *Micromachines (Basel)*. **8** (10) (2017).
26. Warren, K. M., Islam, M. M., Leduc, P. R., Steward, R. 2D and 3D mechanobiology in human and nonhuman systems. *ACS Applied Materials & Interfaces*. **8** (34), 21869 (2016).
27. Pellegata, A. F., Tedeschi, A. M., De Coppi, P. Whole organ tissue vascularization: engineering the tree to develop the fruits. *Front Bioeng Biotechnol*. **6**, 56 (2018).
28. Nguyen, D. H. et al. Biomimetic model to reconstitute angiogenic sprouting morphogenesis in vitro. Proceedings of the National Academy of Sciences of the United States of America. **110** (17), 6712–6717 (2013).
29. Osaki, T., Sivathanu, V., Kamm, R. D. Crosstalk between developing vasculature and optogenetically engineered skeletal muscle improves muscle contraction and angiogenesis. *Biomaterials*. **156**, 65–76 (2018).
30. Ribas, J. et al. Biomechanical strain exacerbates inflammation on a progeria-on-a-chip model. *Small*. **13** (15), 1603737 (2017).
31. Song, J. W., Bazou, D., Munn, L. L. Anastomosis of endothelial sprouts forms new vessels in a tissue analogue of angiogenesis. *Integrative Biology Quantitative Biosciences from Nano to Macro*. **4** (8), 857–862 (2012).
32. Kim, J. et al. Engineering of a Biomimetic Pericyte-Covered 3D Microvascular Network. *PLoS One*. **10** (7), e0133880 (2015).
33 Divito, K. A., Daniele, M. A., Roberts, S. A., Ligler, F. S. & Adams, A. A. Microfabricated blood vessels undergo neoangiogenesis. *Biomaterials.* **138** 142-152 (2017).
34. Lee, V. K. et al. Creating perfused functional vascular channels using 3D bio-printing technology. *Biomaterials*. **35** (28), 8092 (2014).
35. Buchanan, C. F., Verbridge, S. S., Vlachos, P. P., Rylander, M. N. Flow shear stress regulates endothelial barrier function and expression of angiogenic factors in a 3D microfluidic tumor vascular model. *Cell Adhesion & Migration*. **8** (5), 517–524 (2014).
36. Jr, S. R., Tambe, D., Hardin, C. C., Krishnan, R., Fredberg, J. J. Fluid shear, intercellular stress, and endothelial cell alignment. *American Journal of Physiology Cell Physiology*. **308** (8), C657 (2015).
37. Kim, S., Chung, M., Ahn, J., Lee, S., Jeon, N. L. Interstitial flow regulates the angiogenic response and phenotype of endothelial cells in a 3D culture model. *Lab on A Chip*. 4189–4199 (2016).
38. Shirure, V. S., Lezia, A., Tao, A., Alonzo, L. F., George, S. C. Low levels of physiological interstitial flow eliminate morphogen gradients and guide angiogenesis. *Angiogenesis*. (6801), 1–12 (2017).
39. Bazou, D. et al. Flow-induced HDAC1 phosphorylation and nuclear export in angiogenic sprouting. *Scientific Reports*. **6**, 34046 (2016).
40. Vickerman, V., Kamm, R. D. Mechanism of a flow-gated angiogenesis switch: early signaling events at cell–matrix and cell–cell junctions. *Integrative Biology Quantitative Biosciences from Nano to Macro*. **4** (8), 863 (2012).
41. Song, J. et al. Microfluidic platform for single cell analysis under dynamic spatial and temporal stimulation. *Biosens Bioelectron*. **104**, 58–64 (2018).
42. Jeong, G. S. et al. Sprouting angiogenesis under a chemical gradient regulated by interactions with an endothelial monolayer in a microfluidic platform. *Analytical*

Chemistry. **83** (22), 8454–8459 (2011).
43. Steward, R. L., Tan, C., Cheng, C. M., Leduc, P. R. Cellular force signal integration through vector logic Gates. *Journal of Biomechanics*. **48** (4) (2015).
44. Jing, Z., Niklason, L. E. Microfluidic artificial "vessels" for dynamic mechanical stimulation of mesenchymal stem cells. *Integrative Biology Quantitative Biosciences from Nano to Macro*. (12), 1487–1497 (2012).
45. Zheng, W. et al. A microfluidic flow-stretch chip for investigating blood vessel biomechanics. *Lab on A Chip.* **12** (18), 3441-3450 (2012).
46. Buchanan, C. F. et al. Three-dimensional microfluidic collagen hydrogels for investigating flow-mediated tumor-endothelial signaling and vascular organization. *Tissue Engineering Part C Methods*. **20** (1), 64 (2014).
47. Pries, A. R., Secomb, T. W., Gaehtgens, P. Biophysical aspects of blood flow in the microvasculature. *Cardiovascular Research*. **32** (4), 654–667 (1996).
48. Zhao, P. et al. Flow shear stress controls the initiation of neovascularization via heparan sulfate proteoglycans within biomimic microfluidic model. *Lab on A Chip*. **21**, 421–434 (2021).
49. Yamamura, N., Sudo, R., Ikeda, M., Tanishita, K. Effects of the mechanical properties of collagen gel on the in vitro formation of microvessel networks by endothelial cells. *Tissue Engineering*. **13** (7), 1443 (2007).
50. Huxley, V. H., Curry, F. E., Adamson, R. H. Quantitative fluorescence microscopy on single capillaries: alpha-lactalbumin transport. *American Journal of Physiology*. **252** (1 Pt 2), H188 (1987).
51. Kim, S., Lee, H., Chung, M., Jeon, N. L. Engineering of functional, perfusable 3D microvascular networks on a chip. *Lab on A Chip*. **13** (8), 1489–1500 (2013).
52. Campisi, M. et al. 3D self-organized microvascular model of the human blood-brain barrier with endothelial cells, pericytes and astrocytes. *Biomaterials*. **180**, 117–129 (2018).
53. Polacheck, W. J. et al. A non-canonical Notch complex regulates adherens junctions and vascular barrier function. *Nature*. **552** (7684), 258–262 (2017).
54. Nguyen, D. H. et al. Biomimetic model to reconstitute angiogenic sprouting morphogenesis in vitro. *Proceedings of the National Academy of Sciences of the United States of America*. **110** (17), 6712–6717 (2013).
55. Huang, C. P. et al. Engineering microscale cellular niches for three-dimensional multicellular co-cultures. *Lab on A Chip*. **9** (12), 1740–1748 (2009).
56. Chung, M., Ahn, J., Son, K., Kim, S.,Jeon, N. L. Biomimetic model of tumor microenvironment on microfluidic platform. *Advanced Healthcare Materials*. **6** (15) (2017).
57. Kakisis, J., Liapis, C., Sumpio, B. Effects of cyclic strain on vascular cells. *Endothelium*. **11** (1), 17–28 (2004).
58. Charoenpanich, A. et al. Cyclic tensile strain enhances osteogenesis and angiogenesis in mesenchymal stem cells from osteoporotic donors. *Tissue Engineering Part A*. **20** (1–2), 67–78 (2014).
59. Narimiya, T. et al. Orthodontic tensile strain induces angiogenesis via type IV collagen degradation by matrix metalloproteinase. *Journal of Periodontal Research*. **52** (5) (2017).

793

Figure

Click here to access/download;Figure;Figure-1.tif

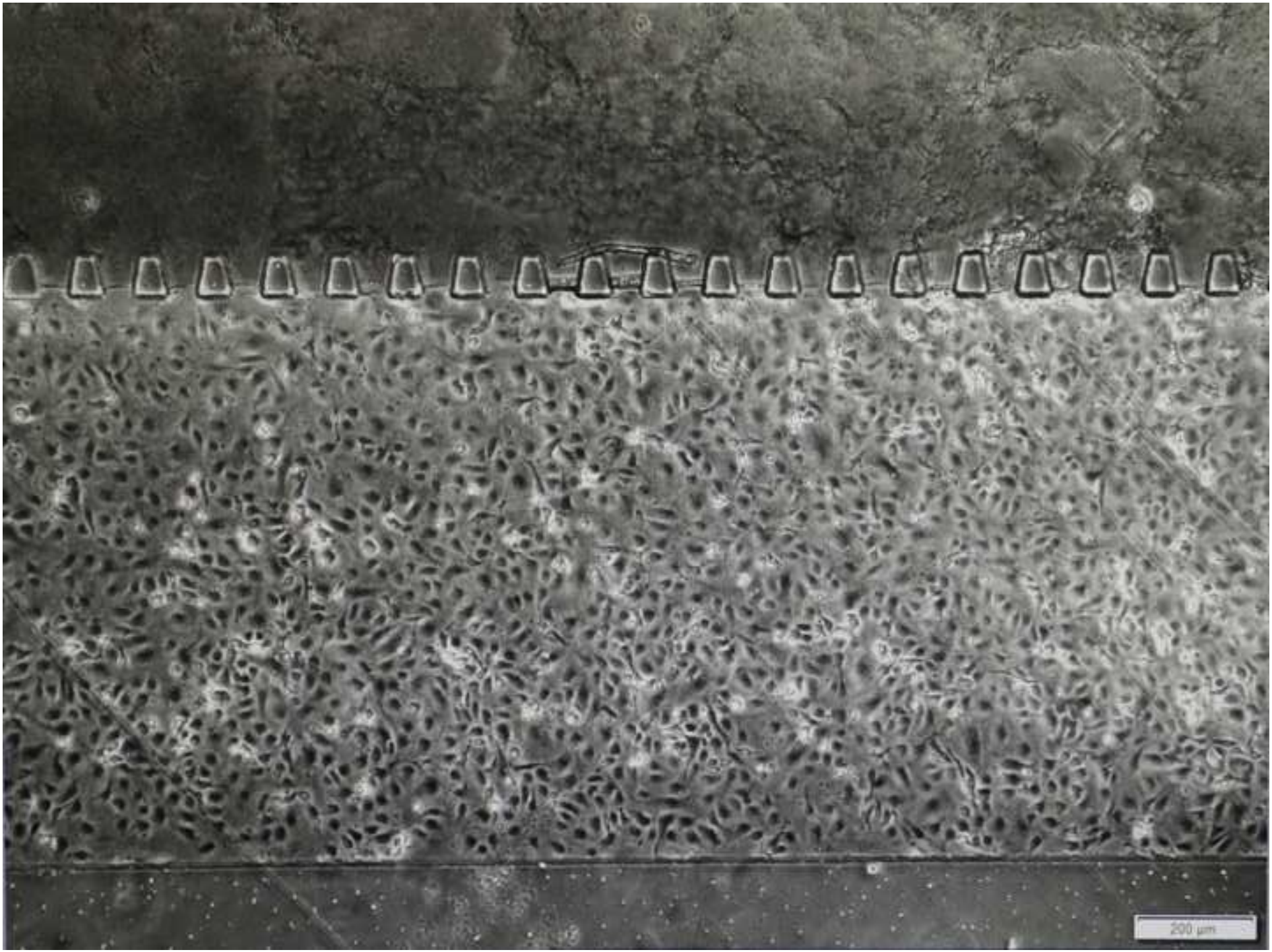

Figure

Click here to access/download;Figure;Figure-2.tif

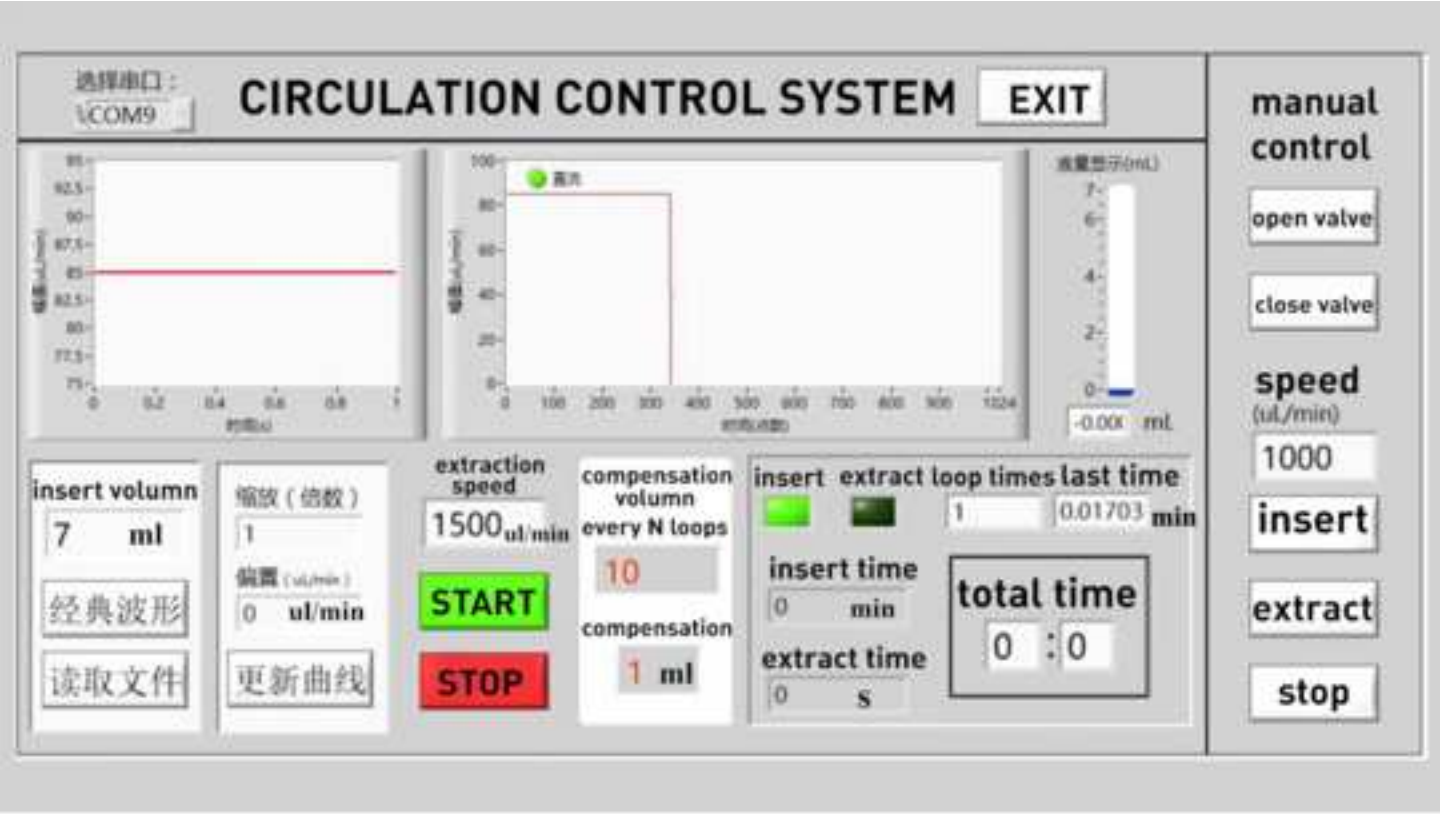

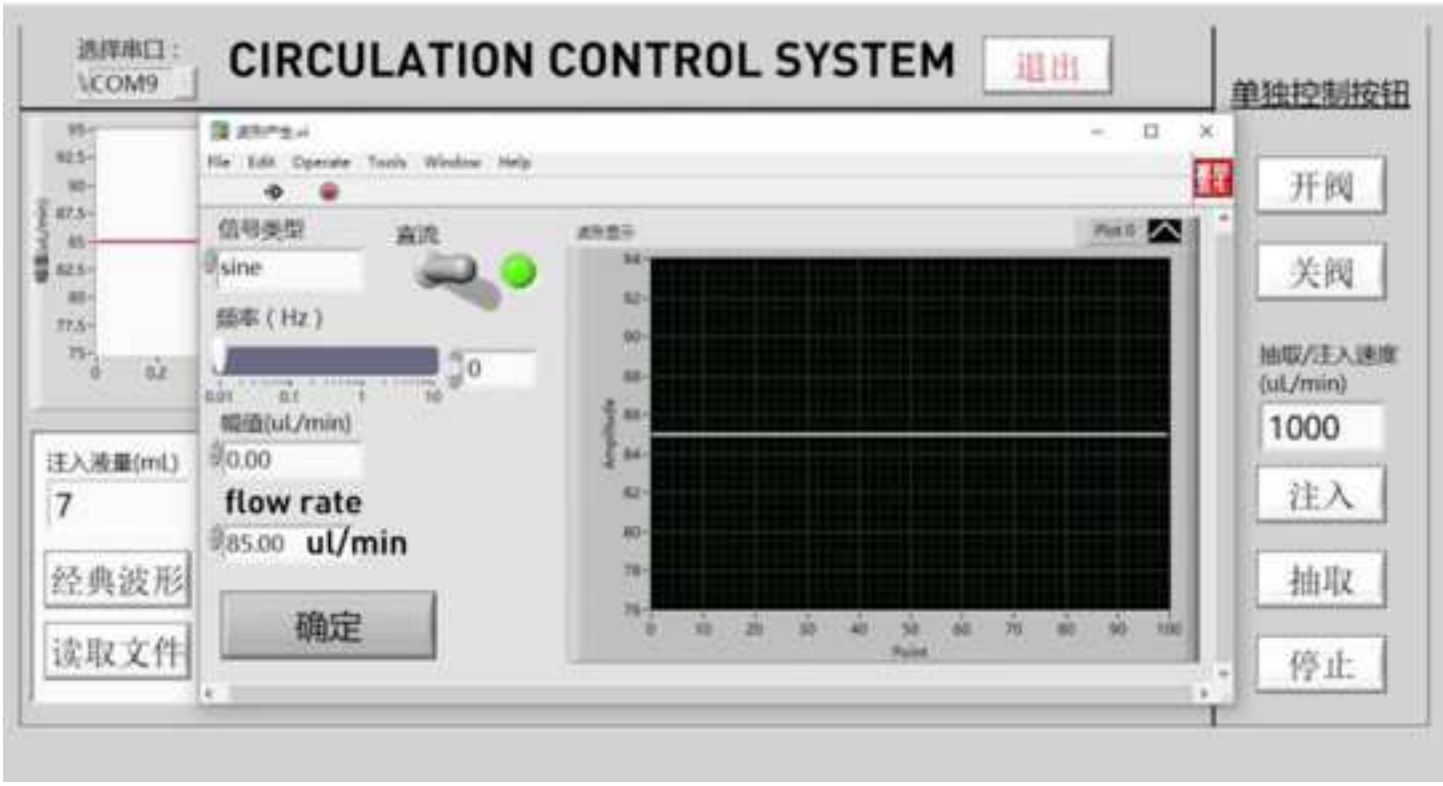

Figure

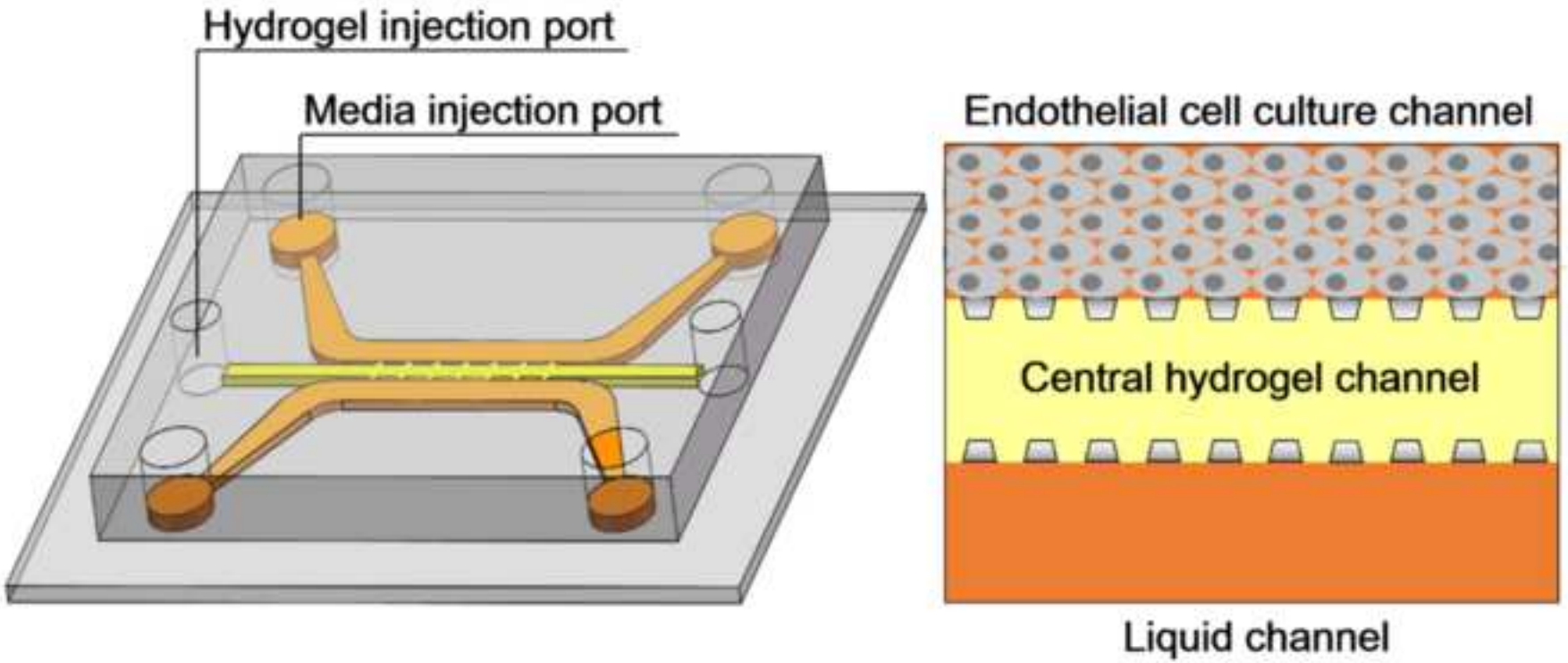

Figure

Click here to access/download;Figure;Figure-4.tif

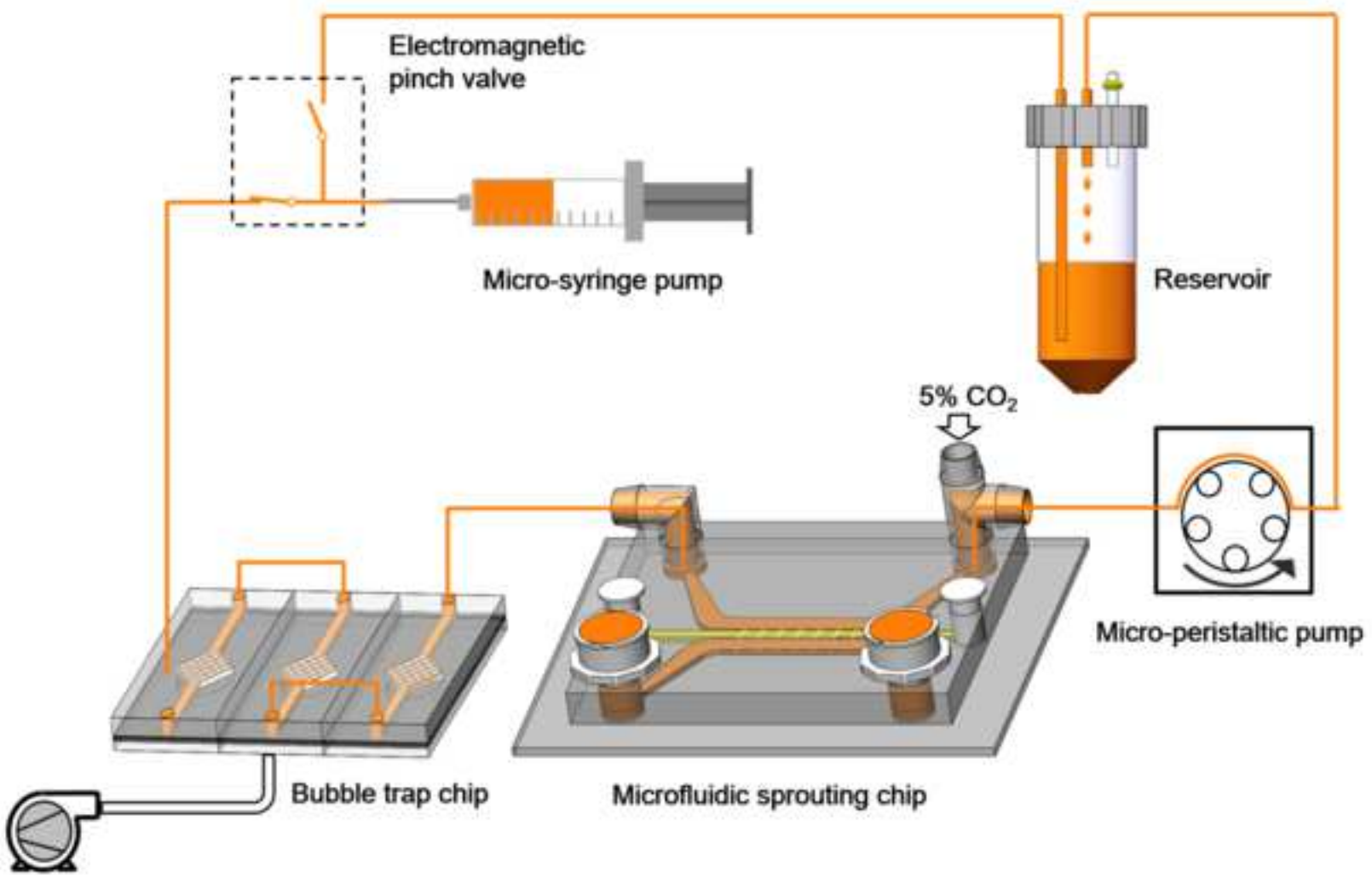

Figure

Click here to access/download;Figure;Figure-5.tif

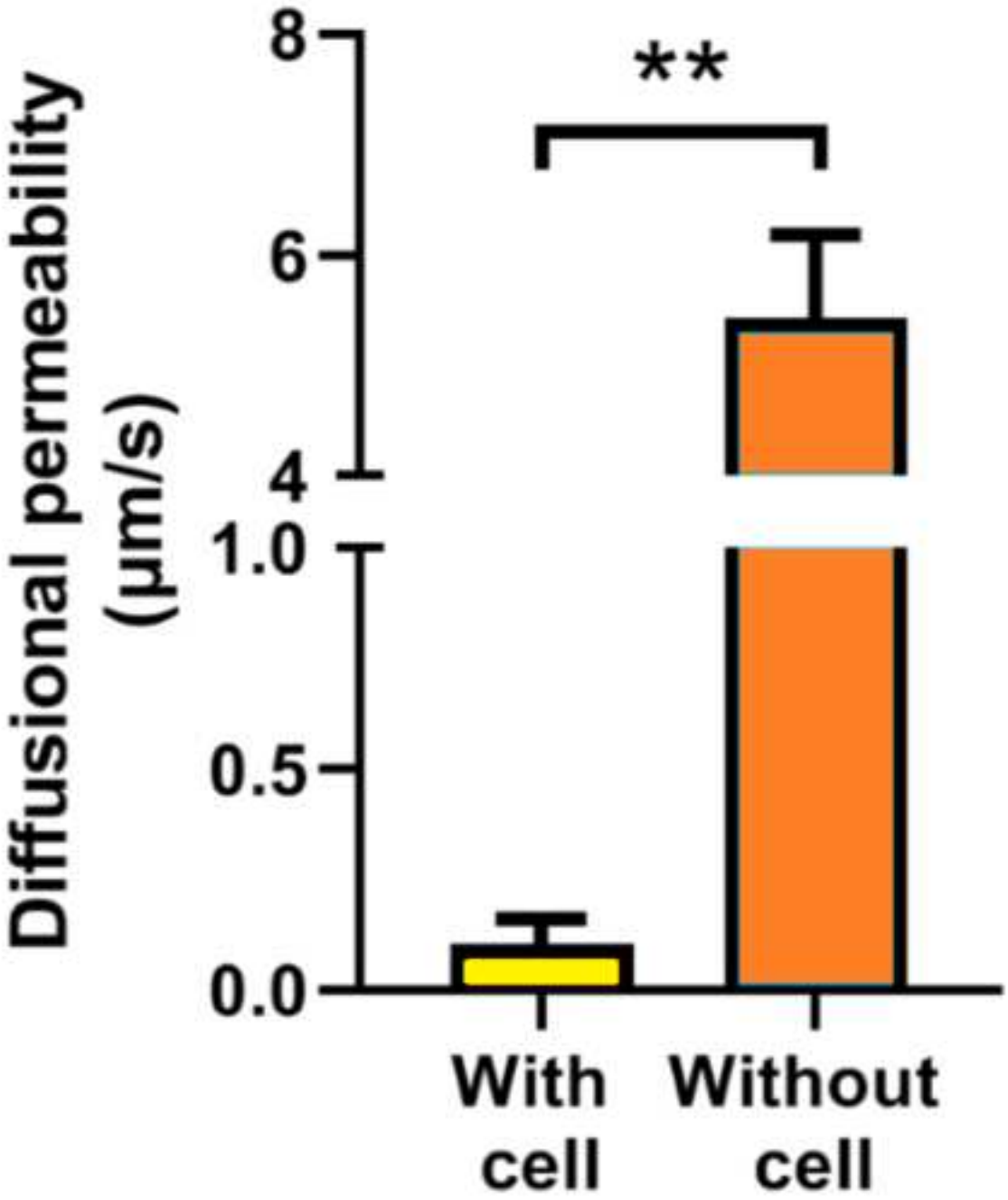

Figure

Click here to access/download;Figure;Figure-6.tif

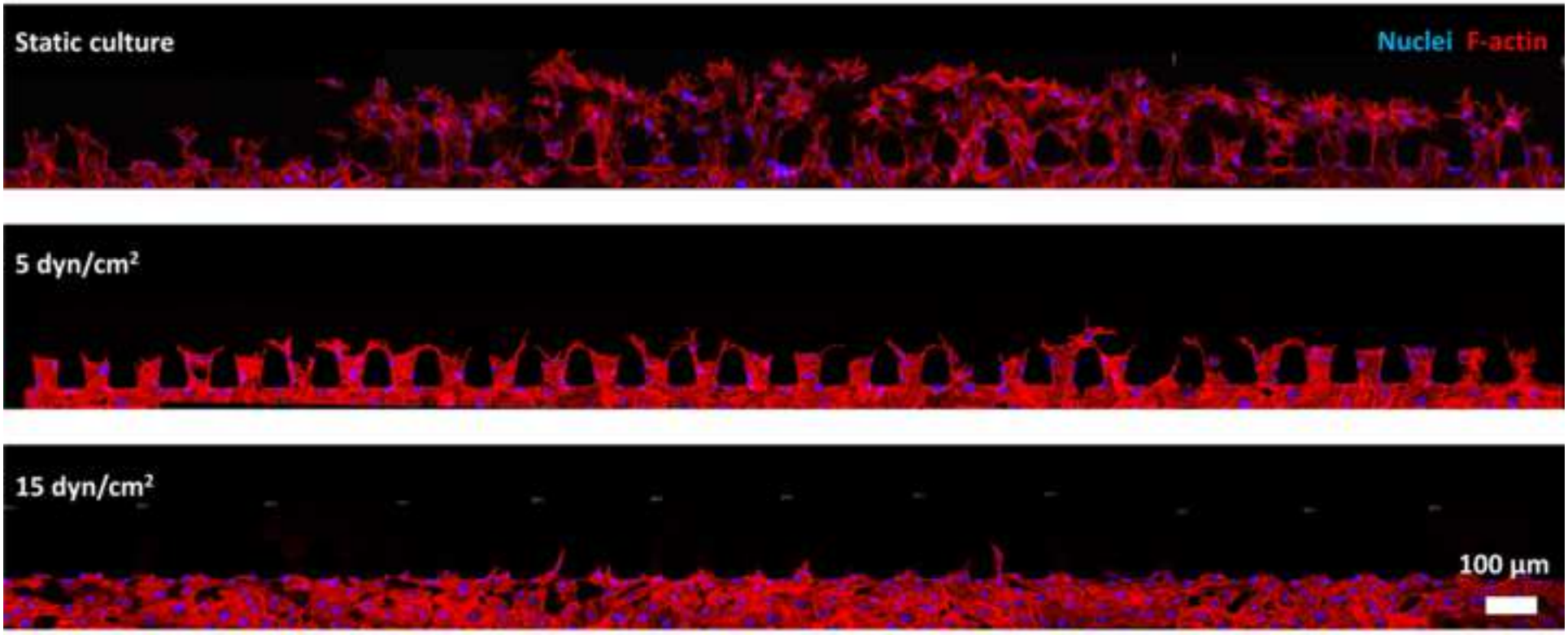

Figure

Click here to access/download;Figure;Figure-7.tif

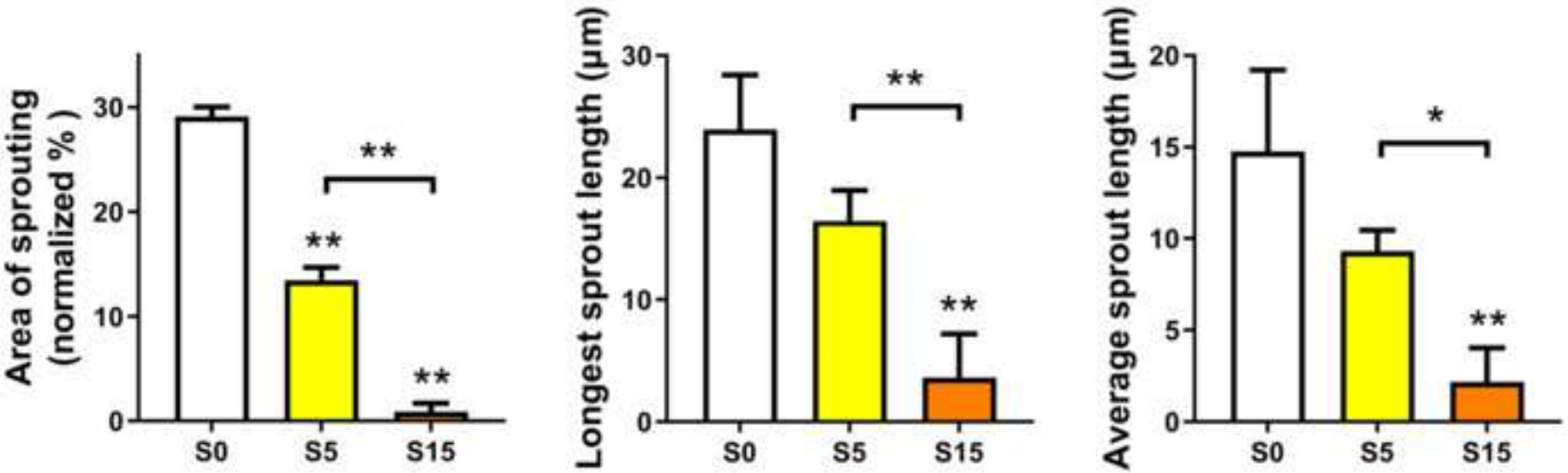

Name of Material/ Equipment	Company	Catalog Number
0.25% Trypsin-EDTA	Genview	GP3108
Collagen I, rat tail	Corning	354236
DAPI	Sigma-Aldrich	D9542
Electromagnetic pinch valve	Wokun Technology	WK02-308-1/3
Endothelial cell medium (ECM)	Sciencell	1001
Fetal bovine serum (FBS)	Every Green	NA
Fibronectin	Corning	354008
FITC-dextran	Miragen	60842-46-8
Graphical programming environment	Lab VIEW	NA
Image editing software	PhotoShop	NA
Image processing program	ImageJ	NA
Isopropanol	Sigma-Aldrich	91237
Lithography equipment	Institute of optics and electronics, Chinese academy of sciences	URE-2000/35
Methanol	Sigma-Aldrich	82762
Micro-peristaltic pump	Lead Fluid	BT101L
Micro-syringe pump	Lead Fluid	TYD01
Oxygen plasma	MING HENG	PDC-MG
Paraformaldehyde	Sigma-Aldrich	P6148
PBS (10x)	Beyotime	ST448
Permanent epoxy negative photoresist	Microchem	SU-8 2075
Phenol Red sodium salt	Sigma-Aldrich	P5530
Polydimethylsiloxane (PDMS)	Dow Corning	Sylgard 184
Poly-D-lysine hydrobromide (PDL)	Sigma-Aldrich	P7886
Polytetrafluoroethylene	Teflon	NA
Program software	MATLAB	NA
Recombinant Human VEGF-165	StemImmune LLC	HVG-VF5
Sodium hydroxide (NaOH)	Sigma-Aldrich	1.06498
Stage top incubator	Tokai Hit	NA
SU-8 developer	Microchem	NA
Trichloro(1H,1H,2H,2H-perfluorooctyl)silane	Sigma-Aldrich	448931
TRITC Phalloidin	Sigma-Aldrich	P5285

Response to Editor

All page numbers and line numbers refer to the file '*Revised Manuscript (marked)*'

Response to Editor

Comment 1:

Please move the scripting language from step 8.3/8.4 to a supplemental file.

Response 1:

We moved the codes from step 8.3/8.4 to the supplemental file.

Comment 2:

Please spell out all journal titles.

Response 2:

We corrected the journal to its full name.

Video Comment 1:

Typos:

- 01:08 Reservior should be spelled "Reservoir"
- 01:08 Microfiudic should be spelled "Microfluidic"
- 09:26 Conclution (should be spelled Conclusion)"

Response 1:

Thanks for the editor's suggestion. We corrected the spelling mistakes from the video.

Important correction:

The affiliations of the authors are corrected according to the new rules of the school in this new term and the request of the authors. We corrected the information in both the manuscript and video. In addition, we found that Xiao Liu was lost from the corresponding author list in the manuscript and was added in the revised manuscript.